

Quantum Features in Atomic Nanofabrication using Exactly Resonant Standing Waves

Dirk Jürgens,^{1,*} Alexander Greiner,¹ Ralf Stützle,² Anja Habenicht,¹ Edwin te Sligte,^{1,†} and Markus K. Oberthaler²

¹Fachbereich Physik, Universität Konstanz, Fach M696, 78457 Konstanz, Germany

²Kirchhoff-Institut für Physik, Universität Heidelberg, Im Neuenheimer Feld 227, 69120 Heidelberg, Germany[‡]

(Received 26 January 2004; published 29 November 2004)

We report on the first fabrication of nanostructures with exactly resonant light revealing the quantum character of the atom-light interaction. Classically the formation of nanostructures is not expected; thus, the observed formation of complex periodic line patterns can be explained only by treating atom-light interaction *and* propagation of the atoms quantum mechanically. Our numerical quantum calculations are in *quantitative* agreement with this experimental finding. Moreover, the theory predicts that for small detunings nanostructures with $\lambda/4$ period can be produced, which beats the standard nanofabrication limit of $\lambda/2$. Our experiments confirm this prediction.

DOI: 10.1103/PhysRevLett.93.237402

PACS numbers: 78.67.-n, 03.75.Be, 42.50.Vk, 81.16.-c

The ability to control the motion of atoms utilizing the atom-light interaction has led to new fundamental physics such as laser cooling [1], Bose-Einstein condensation [2], and precision experiments [3]. The control of the trajectories of atoms has also found its way to applied science and allows the fabrication of nanostructures [4,5].

The basic idea of atomic nanofabrication is the controlled deposition of atoms on a surface. This is achieved by employing spatially varying light forces, realized in *standard* atomic nanofabrication with off resonant standing light waves. These forces are well described within a classical atom-light interaction model [5]; however, this picture implies that these forces vanish for exactly resonant light fields. Thus no nanostructures are expected, whereas the quantum mechanical treatment of the atom-light interaction predicts the formation of structures for exactly resonant standing light waves. Furthermore, the detailed analysis of the formed pattern reveals that in contrast to the off resonant case the spatial phase of the light field plays a crucial role for the quantum mechanical motion of the atoms. Additionally, this system represents a new method for generating periodic patterns with feature spacing smaller than the periodicity of the light intensity distribution. Introducing a detuning in the order of the natural linewidth periodic nanostructures with doubled periodicity can be fabricated. This adds a new scheme to the previously proposed and demonstrated methods to beat the $\lambda/2$ periodicity limit of standard nanofabrication [6–8].

In our experiments a chromium atomic beam is collimated to a divergence of less than 1 mrad (full width at half maximum) by one-dimensional laser cooling in a lin \perp lin configuration. The atomic beam impinges perpendicular onto the exactly resonant standing light wave (${}^7S_3 \rightarrow {}^7P_4$ at $\lambda = 425.6$ nm) which is realized by retro-reflecting a linearly polarized Gaussian laser beam (waists $w_z = 21 \pm 3$ μm and $w_y = 35 \pm 3$ μm , power $P = 17 \pm 2$ mW) from a mirror. Thus the interaction time of the atoms with a mean longitudinal velocity $v_z =$

1000 m/s is on the order of the natural lifetime of the excited state. After traversing the light field, the chromium atoms are deposited on a silicon substrate which is placed 35 ± 5 μm behind the center of the standing light wave in order to reduce diffraction effects from the substrate edge [9]. After 30 min of deposition, the sample is taken out of the high vacuum chamber and analyzed with an atomic force microscope (AFM). In Figs. 1(c) and 1(d) the topography of the fabricated nanostructure is shown. The image consists of 42 overlapping AFM scans reveal-

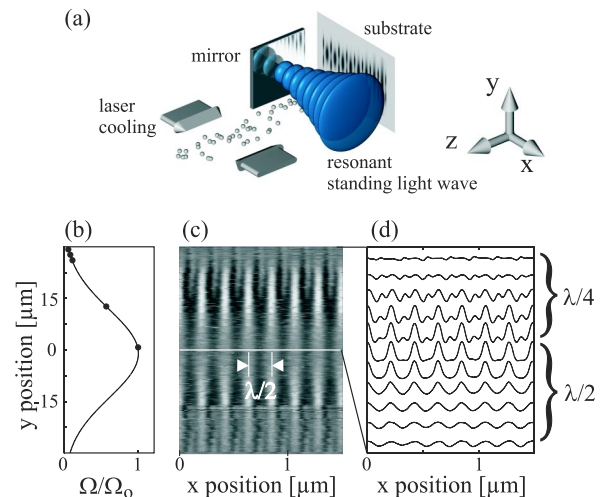


FIG. 1 (color online). Experimental setup and results. (a) A collimated chromium beam impinges on a resonant standing light wave and subsequently hits a substrate. After deposition the substrate topography is analyzed with an atomic force microscope (AFM). (b) The Rabi frequency shows a spatial dependence due to the Gaussian laser beam profile along the y direction. Thus each individual substrate contains the whole intensity dependence of the atom-light interaction. (c) The AFM image and (d) cross sections reveal the light intensity dependence of the formed structures. For low intensity, peculiar periodic structures with feature spacings below $\lambda/2$ are observed.

ing the topography over $60 \mu\text{m}$ in the y direction. Because of the Gaussian profile of the light field in the y direction [see Fig. 1(b)], this image shows the full intensity dependence of the focusing properties of the resonant standing light wave.

The measured topography reveals that for high light intensities nanostructures with a periodicity of $\lambda/2$ corresponding to 213 nm are produced. This is the same result as obtained with an off resonant standing light wave, although in our experiment there is no force expected in the classical atom-light interaction picture. For smaller intensities a striking complex periodic line pattern is produced, which reveals lines spaced at 213 nm and additional features in between. We show that this feature can be attributed to the quantum nature of the atom-light interaction and of the atomic propagation.

First we give a qualitative discussion of the obtained experimental results in the framework of dressed states. We then discuss our quantum mechanical simulations which even allow a quantitative comparison between theory and experiment.

Dressed states are the eigenstates of the coupled atom-light system and are superpositions of the eigenstates of the uncoupled atom $|g\rangle$ and $|e\rangle$. In the exactly resonant case the dressed states and their energy are very simple [10] and are given by

$$|\pm; \mathbf{r}\rangle = \frac{1}{\sqrt{2}}(e^{-i\varphi(\mathbf{r})/2}|g\rangle \pm e^{i\varphi(\mathbf{r})/2}|e\rangle),$$

$$E_{\pm}(\mathbf{r}) = \pm \frac{\hbar}{2}|\Omega(\mathbf{r})|,$$

where the atom-light coupling is characterized by the complex Rabi frequency $\Omega = -\mathbf{d} \cdot \mathbf{E}(r)/\hbar = |\Omega(r)|e^{i\varphi(r)}$, \mathbf{d} is the atomic electric-dipole moment, and \mathbf{E} represents the electric field amplitude of the light field.

For a perfect standing light wave, the dressed states are degenerate at the nodes where the electric field vanishes and thus $E_+ = E_- = 0$. This degeneracy is lifted in our experiment, because we use a mirror with a reflectivity of $R = 94\%$. The corresponding intensity distribution and resulting complex Rabi frequency is depicted in Fig. 2(a). It is important to note that the phase of the Rabi frequency changes dramatically at the nodes of the standing light wave that breaks the symmetry of the light field there. In Fig. 2(b) the corresponding dressed state energies are shown and the motion of a ground state atom is indicated.

In the regions where the Rabi frequency has a weak phase dependence the evolution of a ground state atom is given by the corresponding dressed states, whose motions are governed by Newton's equations of motion resulting from the corresponding potential E_+ and E_- . In standard nanofabrication utilizing far off resonance light forces the ground state atom is very well described by only *one* dressed state (blue detuning mainly $|+\rangle$). But in an

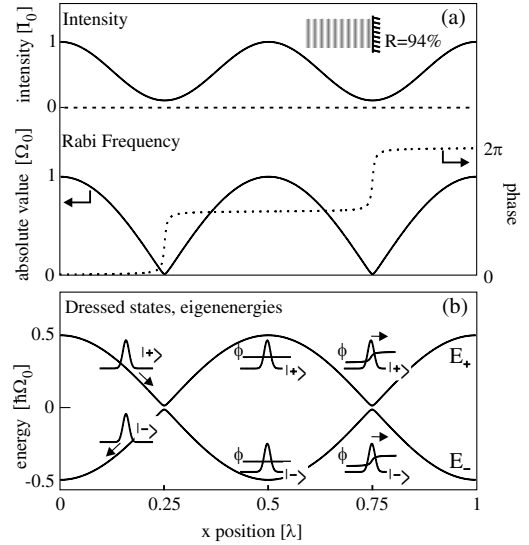


FIG. 2. Dressed states description of on resonant atom-light interaction: (a) The standing light wave is formed by retro-reflecting a laser beam from a mirror with reflectivity $R = 94\%$ as shown in the inset. This leads to a periodic intensity distribution that is not fully modulated (depicted not to scale). Hence, the Rabi frequency is complex. The change in phase proves to be dramatic at the standing wave node, where the phase jumps by π within few nanometers. (b) Where the phase is constant, the ground state wave packet is decomposed into two resting dressed state wave packets, whereas near the nodes this decomposition leads to two moving dressed state wave packets. Their motion is deduced from the dressed state eigenenergies, therefore a $|+\rangle$ -state wave packet is attracted to the node and a $|-\rangle$ -state wave packet to the antinode of the standing wave. As illustrated at position $x = 0.75$, the motion of wave packets near the node is influenced less by the potentials and more by the phase gradient of the Rabi frequency.

exactly resonant light field a ground state atom is described as a *fifty-fifty* superposition of the two dressed states $|+\rangle$ and $|-\rangle$. Thus an atomic wave packet in a light field gradient will split into two parts. The $|-\rangle$ is attracted to the intensity maxima while the $|+\rangle$ state is pulled to the intensity minima as indicated in Fig. 2(b). This splitting is known as the optical Stern Gerlach effect [11] and has already been observed by looking at the momentum distribution [12]. In our experiment we directly observe this effect by detecting the atomic position on the nanometer scale.

The motion in the $|-\rangle$ -state potential is almost perfectly harmonic close to its minimum and concentrates the atoms like a lens for matter waves. This is very similar to the standard atomic nanofabrication schemes. The $|+\rangle$ -state potential has a triangular shape in the vicinity of its minimum and corresponds to an atom optical axicon, which produces a focal line. Since the distance between adjacent $|+\rangle$ -state and $|-\rangle$ -state potential minima is $\lambda/4$, nanostructures with half the standard periodicity limit of $\lambda/2$ are expected.

The experimental observation that these $\lambda/4$ structures are not found for high light intensity can easily be understood by realizing that nonadiabatic (NA) transitions between the dressed states can happen near the nodes. The probability for a NA transition is estimated as discussed in [10]. It is found that the reflectivity must be chosen smaller than 50% to suppress NA transitions and allow for the atoms to oscillate around the potential minima of the $|+\rangle$ state. For our high reflectivity of $R = 94\%$ the NA transition probability is almost unity. However, for interaction times shorter than a quarter of an oscillation time in the axicon potential, which depends on the light intensity, a localization at both nodes and antinodes can be expected. Thus the simple dressed state potential picture explains why in the high intensity region only $\lambda/2$ structures are observed, whereas it fails to explain the observed complex pattern for low light intensity shown in Figs. 1(d) and 3(b).

The so far discussed semiclassical description of the motion is correct only for light fields with vanishing phase gradients. But near the node, where the phase of the Rabi frequency changes rapidly, the simple potential treatment is not applicable. Nevertheless, the dressed state picture allows one to understand the position of the lines formed near the nodes of the standing light wave qualitatively. As indicated in Fig. 2(b) a resting atomic ground state wave packet at the light field node is described in the dressed state basis by a coherent superposition of two

dressed state wave packets moving in the same direction with a momentum $mv = \hbar/2\nabla\phi$. For our experimental situation we estimate the velocity of these wave packets to be $\sim 26v_r$ where $v_r = \hbar k/m = 1.8$ cm/s is the recoil velocity and k is the wave number of the light. Thus one expects that atoms in the $|+\rangle$ state near the node run up the potential due to this velocity [indicated in Fig. 2(b)]. An estimate of the expected shift after a certain time can be found by calculating the classical trajectory of a particle starting at the node with an initial velocity $\sim 26v_r$ in the linear potential $V(x) = \hbar k|\Omega|x/2$. For the interaction time of 40 ns and a Rabi frequency of $|\Omega| = 20\Gamma$ we find the position to be shifted by 14 nm from the node. Experimentally we observe 12 ± 3 nm. This effect is very closely connected to the scattering force [11] commonly applied in laser cooling. There the situation is usually much simpler since the populations of the dressed states can be assumed to be in steady state, while in our experiment this is not the case.

Therefore to understand our experimental findings quantitatively we numerically solve the Schrödinger equation for the two-level atom in momentum space [13]. Here, the two-level approach is reasonable as long as the intensive linearly polarized light field defines the quantization axis and thus couples only magnetic substates with equal quantum number ($\Delta m = 0$). This is strictly speaking not true near the nodes. Therefore we numerically calculated the eigenenergies near the intensity minimum including the earth magnetic field for arbitrary directions. We find that the resulting eigenenergies are always symmetric with respect to the node of the standing light wave. Additionally the spatial range where anticrossings [6] between a few of the involved energy levels occur is ± 4 nm, which is the region where the dynamics is governed anyway by NA transitions. In order to get a quantitative agreement between the experimental findings and the numerical solution we include the effect of spontaneous emissions empirically. According to the dressed state analysis given in [10], spontaneous emissions can change the dressed state leading to momentum diffusion due to the instantaneous sign reversal of the dipole force (the recoil kick of the emitted photon is negligible). After the interaction time t this momentum diffusion translates into a feature broadening $\Delta x(\Omega) \propto v_r \Omega t / \Gamma$. To account for this broadening a convolution of the calculated spatial probability distribution (taking into account the divergence of the beam) with a Gaussian of width $\Delta x(\Omega)$ is applied. This convolution is important only at high light intensities while it does not significantly influence the structure shape at low light intensities. The additional broadening effect due to the growth behavior of Cr [9] is negligible for our broad structures (70 nm).

Cross sections of the calculated atomic flux at a distance of $35 \mu\text{m}$ behind the center of the standing wave

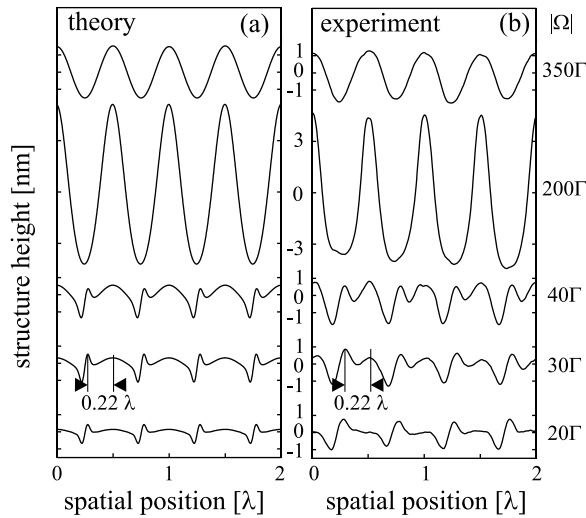


FIG. 3. (a) Cross sections of the calculated atomic flux at a distance of $35 \mu\text{m}$ behind the center of the standing wave for the indicated Rabi frequencies. For large Rabi frequencies, $\lambda/2$ period nanostructures are formed, whereas low Rabi frequencies lead to peculiar patterns with feature spacings smaller than $\lambda/2$. (b) AFM cross sections taken at different positions as indicated with solid circles in Fig. 1(b) corresponding to equivalent Rabi frequencies as used in the quantum simulation. The experimental findings are in excellent quantitative agreement with the simulation.

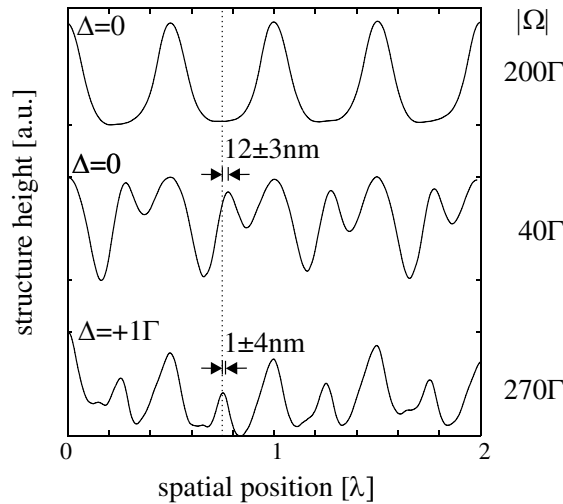


FIG. 4. Comparison between nanostructures fabricated with different detunings: For $\Delta = 0$, $\lambda/2$ structures are shown to illustrate the shift of 12 ± 3 nm of the new feature in between. The nanostructures obtained by detuning the laser frequency $\Delta = 1\Gamma$ exhibit a much smaller shift of 1 ± 4 nm. The observed behavior confirms the prediction of our quantum simulation and demonstrate the periodicity doubling for very near resonant standing light waves.

are shown in Fig. 3(a) and compared to the experimental findings shown in Fig. 3(b). The experimental cross sections are taken at positions indicated in Fig. 1(b) with solid circles. The theoretical curves shown are obtained for the indicated Rabi frequencies. These values are consistent within the uncertainty of the independently measured incoming power and beam waists. Furthermore, we take into account the internal magnetic substructure of chromium by multiplying the calculated Rabi frequency by a factor of 0.65 (average Clebsch-Gordan coefficient for linear polarization), assuming equally populated substates. This is valid in our case because the atoms travel 1 m in a magnetically unshielded region before they enter the focusing region. The simulated flux is in very good agreement with the experimental finding for all Rabi frequencies, and especially the peculiar structure shape is very well reproduced. It is important to note that the structure width and height at high Rabi frequencies are dominated by the momentum diffusion resulting from spontaneous emission.

Our simulations predict that for small blue detuning $\Delta = 1\Gamma$ of the standing light wave the production of nanostructures with a period of $\lambda/4$ is possible. Our results are similar to the reported periodicity reduction by Gupta *et al.* [6], where the chromium specific polarization dependence of the atom-light interaction was utilized. Another method using a Raman configuration consisting of two pairs of counterpropagating traveling wave fields has also been put forward to realize optical potentials with $\lambda/8$ periodicity [8]. Our experimental

findings are shown in Fig. 4, where we compare $\lambda/2$ focusing in the high intensity limit with the low intensity focusing for exactly on resonance and detuned $\Delta = 1\Gamma$ standing light wave. The observed shift for exactly resonant standing light waves of 12 ± 3 nm is in excellent agreement with the theoretical prediction of 12.7 nm. In the detuned case the theory predicts 0.7 nm which is also consistent with the measured shift of 1 ± 4 nm deduced from the pattern shown in Fig. 4.

In conclusion, we have shown that exactly resonant light waves employed in an atomic nanofabrication scheme lead to new complex nanostructures. We are able to attribute the unexpected atomic distribution found on the substrate to the presence of the phase gradient of the resonant light field near its nodes. Our quantum simulations confirm our observations quantitatively. We have also shown that the $\lambda/2$ periodicity limit of conventional atomic nanofabrication schemes can be improved by a factor of 2 using standing light waves with a detuning on the order of the natural linewidth.

We thank J. Mlynek for his generous support, and O. Maragò for many fruitful discussions. This research is funded by the SFB513 and Emmy Noether program of the Deutsche Forschungsgemeinschaft, and the Optik-Zentrum in Konstanz and by the RTN network “Cold quantum gases” under Contract No. HPRN-CT-2000-00125.

*Electronic address: dirk.juergens@uni-konstanz.de

†Permanent address: Eindhoven University of Technology, P.O. Box 513, 5600MB Eindhoven, The Netherlands.

‡Electronic address: www.kip.uni-heidelberg.de/matterwaveoptics

- [1] S. Chu, C. N. Cohen-Tannoudji, and W. D. Phillips, *Rev. Mod. Phys.* **70**, 685 (1998).
- [2] W. Ketterle, *Rev. Mod. Phys.* **74**, 1131 (2002).
- [3] T. L. Gustavson, P. Bouyer, and M. A. Kasevich, *Phys. Rev. Lett.* **78**, 2046 (1997).
- [4] G. Timp *et al.*, *Phys. Rev. Lett.* **69**, 1636 (1992).
- [5] D. Meschede and H. Metcalf, *J. Phys. D* **36**, R17 (2003); M. K. Oberthaler and T. Pfau, *J. Phys. Condens. Matter* **15**, R233 (2003).
- [6] R. Gupta, J. J. McClelland, P. Marte, and R. J. Celotta, *Phys. Rev. Lett.* **76**, 4689 (1996).
- [7] Th. Schulze *et al.*, *Microelectron. Eng.* **46**, 105 (1999).
- [8] B. Dubetsky and P. R. Berman, *Phys. Rev. A* **66**, 045402 (2002), and references therein.
- [9] W. R. Anderson, C. C. Bradley, J. J. McClelland, and R. J. Celotta, *Phys. Rev. A* **59**, 2476 (1999).
- [10] J. Dalibard and C. Cohen-Tannoudji, *J. Opt. Soc. Am. B* **2**, 1707 (1985).
- [11] R. J. Cook, *Phys. Rev. A* **35**, 3844 (1987).
- [12] T. Sleator *et al.*, *Phys. Rev. Lett.* **68**, 1996 (1992).
- [13] M. A. Efremov, M. V. Fedorov, V. P. Yakovlev, and W. P. Schleich, *Laser Physics* **13**, 995 (2003).